Acta Physica Universitatis Comenianae
Vol. XLVI–XLVII, (2005–2006) 53–64

Cavity Ring-Down Spectrometer New Highly Sensitive Detection Technique at Comenius University in Bratislava

T. Földes, V. Foltin, P. Čermák, P. Veis, P. Lukáč, P. Macko

Department of Experimental Physics, Faculty of Mathematics, Physics and Informatics,
Comenius University, Mlynská dolina F2, 842 48 Bratislava, Slovak Republic
e-mail: *tfoldes@hotmail.com, vfoltin@fmph.uniba.sk, macko@fmph.uniba.sk*

Abstract: We present an experimental setup incorporating a CRDS spectrometer that enables detection of particles with high sensitivity. The performance of the system is demonstrated. We designed and constructed the spectrometer using a diode laser so that it is comparable with setups employing expensive lasers. CRDS applications in plasma physics are outlined.

1. Introduction

Direct absorption spectroscopy of atoms and molecules in the gas phase, yielding either quantitative absolute concentrations or absolute frequency-dependent cross-sections, is a very powerful tool in analytical and physical chemistry. Absoluteness is the reason why sensitive absorption spectroscopic techniques have gained renewed interest even in research fields where more sophisticated laser based diagnostic techniques are commonly applied. In a 'conventional' absorption experiment, the amount of transmitted light through a sample is measured. The attenuation of light due to absorption is described using the Lambert-Beer law [1]

$$I(\ ) \quad {}_0(\ )\exp[\quad (\ )] \tag{1}$$

where $I_0(\ )$ is the light intensity entering the sample, $I(\ )$ is the light intensity exiting the sample, l is the absorption path length through the sample and $(\ )$ is the absorption coefficient of the absorber. Absorption coefficient $(\ )$ is given as $(\ )\quad(\ )$N, where is the absorption cross-section and N is the concentration of concrete particles which is assumed to be constant along l. When is known, absorption spectroscopy is used mainly for determination of N and in the opposite case of known N for determination of . Particles mean particular atoms, molecules and ions in ground or excited states. If the light source is tunable and monochromatic (e.g., a laser), one can record an absorption spectrum of the sample by recording the transmitted intensity as a function of frequency. Alternatively, a broad light source can be used when the incident light or the transmitted light is spectrally dispersed (e.g., in Fourier Transform spectroscopy). A drawback of direct absorption spectroscopy might be its limited sensitivity. A small attenuation of the light intensity has to be measured on the top of a large background. Additionally, intensity fluctuations, for example of a pulsed laser, can be rather large (up to 50 %), thereby obscuring the absorption sig-

nal. Although one can, in principle, correct these pulse-to-pulse fluctuations, significantly better results are obtained when more stable light sources (continuous wave (cw) instead of pulsed) are used. It can be seen from Eq. (1) it can be seen that an increase in the absorption path length results in a stronger absorption signal.

Cavity ring down spectroscopy (CRDS) is an absorption technique in which the sensitivity is primarily improved by increasing the absorption path length using a high finesse optical cavity [2]. The optical cavity is formed by two highly reflective mirrors and acts like a frequency selective filter that transmits light at the frequencies of the cavity eigenmodes. In 'conventional' CRDS spectroscopy light from a pulsed laser is coupled into the cavity and the light inside the cavity is reflected many times between the mirrors. CRDS is a sensitive absorption technique in which the rate of absorption rather than the magnitude of the absorption of a light pulse confined in an optical cavity is measured. Instead of measuring the total intensity of the light exiting the cavity, one determines the decay time by measuring the time dependence of the light leaking out of the cavity. In this way the rate of absorption can be obtained; the more the sample absorbs, the shorter is the measured decay time.

Scheme and equations for "classical" and CRDS optical arrangement:

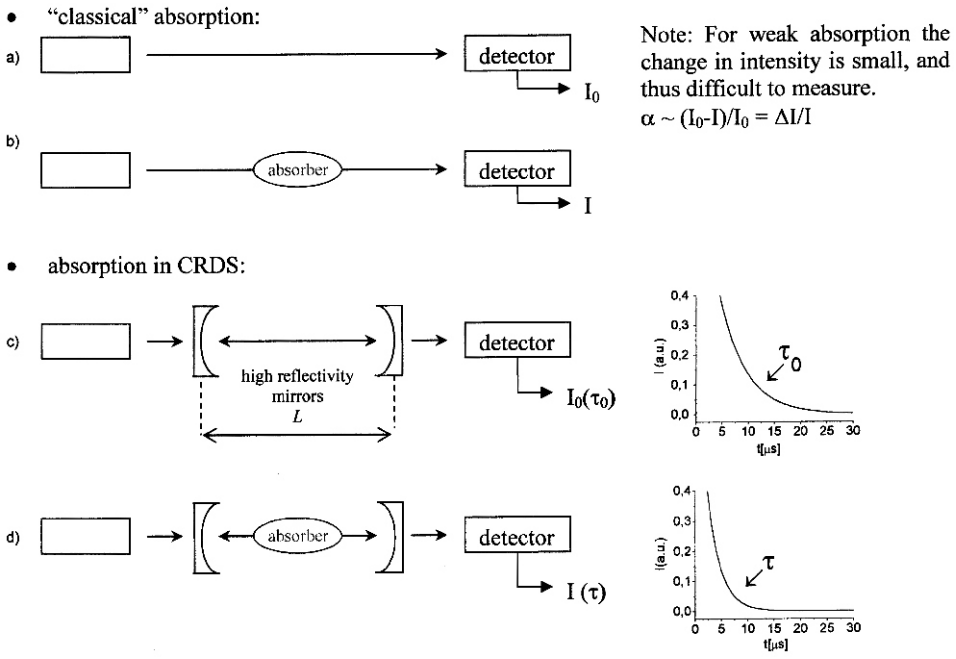

Fig. 1. Schematics of "classical" (a, b) and CRDS (c, d) experiments for absorption.

The intensity of light I(t) leaving the cavity exponentially decreases from the initial intensity I(0) as follows:

$$I(t) \quad I(0)e^{\ t/\ } \quad . \tag{2}$$

From the time constant of the exponential decrease one can find the absorption coefficient of the medium contained in the cavity for a particular wavelength from the following relation:

$$(\ ) \quad \frac{1}{(\ )} \quad \frac{1}{\ _0} \ \frac{L}{cl}. \tag{3}$$

Here L is the length of the resonator, l is the length of absorbing medium, c is the speed of light and $_0$ depends only on reflectivity of mirrors, i.e. on properties of the empty cavity:

$$_0 \quad \frac{L}{c.\ln R} \quad \frac{L}{c(1 \quad R)} \tag{4}$$

with R standing for the coefficient of mirror reflectivity.

Important issues and advantages of the CRDS:

When the laser is tuned to a wavelength at which the sample absorbs and the values of the time constant of the empty and full cavity are determined, one can compute the concentration of the sample. The result depends only on time constants, absorption cross sections and the speed of light. This means that for determining concentration a calibration sample is not needed. CRDS is an absolute measuring method.

A further important property of CRD spectroscopy is the increase of interaction length of sample with the laser beam by a factor of $[n(1 \quad R)]^{\ 1}$ owing to the multiple reflections from the mirrors. Here n is the number of mirrors and R is their reflectivity. For typical mirrors this factor reaches values from 1000 to 100000 in the range of wavelengths from 1500–1600 nm.

Measuring the time constants and not ratios of intensities makes this method immune against fluctuation of the laser.

Since the absorption is determined from the time behaviour of the signal, it is independent of: pulse-to-pulse fluctuations of the laser; the intensity of the laser.

CRDS measurement is a technique with a high sensitivity.

The highest reported sensitivity with pulsed CRDS has been $5\times10^{\ 10}$ cm ^{1}Hz $^{1/2}$ [3].

The sensitivities are higher with cw-CRDS (using continuous wave lasers) than with pulsed CRDS; the highest reported sensitivity was $8.8\times10^{\ 12}$cm $^{\ 1}$ Hz $^{1/2}$ [4]. However, here the coupling of light into the cavity is more difficult [5].

The effective absorption path length, which depends on the reflectivity of the cavity mirrors, can be very long (up to several kilometers), while the sample volume can be kept rather small.

Attractive property of CRDS is simplicity; it is rather easy to construct a CRDS setup using only a few components.

Applications of CRDS:

To date, the CRDS technique has been successfully applied in various environments. High resolution spectroscopy studies have been performed on molecules in cells and supersonic jets and on transient molecules generated in discharges, flow reactors and flames. The CRDS spectra directly provide the frequency-dependent absorption strengths of the molecules under study, which contain information on the number density, cross-sec-

tion and temperature. As long as mirrors with a sufficiently high reflectivity, detectors with a sufficiently fast time response, and tunable (pulsed) light sources are available, there is no intrinsic limitation to the spectral region in which CRDS can be applied. By now, successful application of CRD spectroscopy has been demonstrated from the ultraviolet (UV) part of the spectrum to the infrared (IR) spectral region. Although nowadays most CRDS experiments are performed with pulsed lasers, several schemes have been developed during the last decade in order to perform CRD spectroscopy with cw lasers.

Advantages of continuous-wave cavity ring down spectroscopy (cw-CRDS) are a better spectral resolution and a better duty cycle. Furthermore, the sensitivity of cw-CRDS can, in principle, be improved by careful design of the coupling of the laser modes to the cavity modes. It is interesting to note that the first two cw-CRDS experiments, which have been reported, are inspired by the aforementioned 'precursor' experiments. Engeln *et al.* reported phase shift CRD spectroscopy, in which the absorption spectrum is extracted from a measurement of the magnitude of the phase shift that an intensity modulated cw light beam experiences upon passage through an optical cavity [6]. Later, Romanini *et al.* used the other approach; the resonant cavity mode is swept over the cw laser line, when sufficient light is coupled into the cavity the laser is switched off, and, subsequently, the CRDS transient is recorded [5].

Excitation of a single longitudinal mode of the ring down the cavity provides the best sensitivity. For pulsed CRD spectroscopy, this implies that a Fourier transform limited pulsed laser should be used in combination with a short cavity [3, 7]. In this case, the length of the cavity (thus the modes) should be scanned simultaneously with the laser wavelength, in order to record a CRDS absorption spectrum. An alternative is the use of cw lasers which have to be switched off in order to observe a ring down transient. The bandwidth of these lasers is very small (typically less than a few MHz), therefore longer cavities can be used, resulting in longer ring down times. In the literature, CRD spectroscopy performed with cw laser is entitled cw-CRD spectroscopy, but it should be realized that this technique is, in fact, not a cw technique at all.

Whether pulsed CRDS or cw-CRDS should be used, depends strongly on the application. Pulsed dye lasers and OPO's can be scanned over a large wavelength region. Furthermore, their power is high enough that non-linear conversion techniques (frequency mixing and Raman shifting) can be used to extend the wavelength region to the ultraviolet and infrared. Continuous wave lasers, on the other hand, can only be scanned over small wavelength regions and are not (yet) available at all wavelength regions. The advantage of cw-CRDS is the higher repetition rate and a higher spectral resolution than achievable with pulsed CRD spectroscopy (the latter is only true for multi-mode excitation of the cavity; when exciting a single mode, the resolution in both cw and pulsed CRD spectroscopy is only determined by the width of the very narrow cavity modes). An additional advantage is an increased energy build-up inside the cavity as the line width of the cw laser decreases. Higher intracavity energy results in higher light intensities on the detector, improving the signal-to-noise ratios on the ring down transients and, therefore, improving the sensitivity. Furthermore, compact, easy to use, and rather inexpensive cw diode lasers that have low power consumption and do not require cooling, can be used, which is, for example, interesting for trace gas detection applications at remote locations.

Since there are so many applications at the present time, in which concentration of species in the range of ppb are measured, we indicate only a list of few selected groups working with CRDS:

Plasma physics:

study of H_3^+ recombination with electrons [8, 9] by Glosik et al.

study of sputter erosion – the key mechanism that places fundamental limitations on ion and plasma thruster life times [10] by A. Yalin at al.

discharge spectroscopy [11] by Romanini and Sadeghi.

Biomedical & Environmental physics, Chemistry & Industry:

study of breath diagnostics – used to measure exhaled markers not invasively [12] by M. Murtz et al. (we note from their Table 1 that e.g. carbonyl sulfide with only 0 10 ppb is detectable in human breath constituents)

study of the trace atmospheric elements [13] by M. Murtz et al.

trace explosive vapor detection using broadly tunable optical parametric oscillator [14] by Jeffrey I. Steinfeld et al.

atmospheric pollutants control by [15] Barbara A. Paldus

food industry applications by [16] Barbara A. Paldus

solving chemical problems using CRDS by D. A. Etkinson [17].

2. Experiment

2.1. Cavity ring down arrangement

The experimental setup is shown in Fig. 2. A fibered butterfly-package DFB laser is connected to a fibered optical isolator and through a fiber-optical beam splitter a single mode fiber delivers approx. 99 % of the laser radiation to an acousto-optical switch and approx. 1 % to a Fabry-Perot etalon. The laser radiation passing through the acousto-optical switch enters the cavity through mode-matching optics and can be rapidly deflected. The cavity is composed of 2 high reflectivity mirrors in a vacuum-tight glass cell. The mirrors are mounted on tilt stages one including a piezo-electric tube for modulating the cavity length. The intensity of the light leaking out of the cavity is measured with an InGaAs photodiode and is used to trigger the acousto-optic switch for deflecting the laser radiation

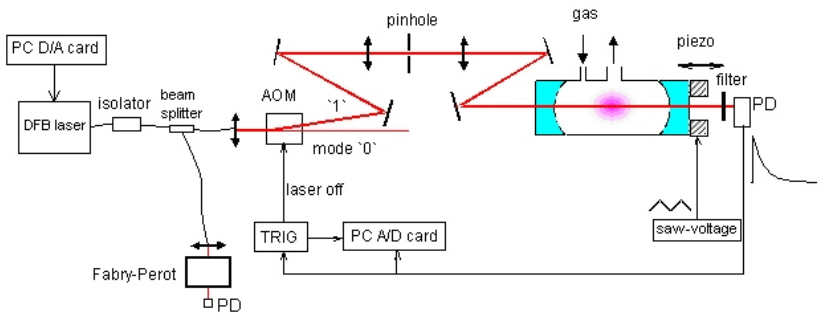

Fig. 2. Schematic diagram of the experimental setup.

and is also on-line analyzed by PC. The length of the cavity is modulated by saw-voltage applied to the piezo-electric tube.

The cavity and all open-air optics are placed on an L-shaped rail, which is lying on a marble tombstone. On-line data analysis, visualization and control of laser tuning are carried out using a PC A/D and a D/A card, employing LabView modules [18].

The reasons to use DFB lasers for a CRDS setup are manifold, despite that they have been, in general, constructed for application in the telecom industry. These lasers are by now available within the entire wavelength range from 730 nm to 2800 nm with output powers between 10 and 150 mW depending on wavelength. All the laser radiation is emitted within a single-mode (TEM00) beam profile. In the laser spectrum, the background of amplified spontaneous emission (ASE) is suppressed relative to the coherent part of the laser radiation by 40 55 dB [19].

The frequency of DFB lasers can be tuned by varying either the operating current, or the temperature of the laser chip. The thermal tuning rate of the DFB lasers is typically 25 30 GHz/K and is comparatively slow (typically 1 nm/s) however, large mode-hop free tuning ranges can be attained. Much faster frequency tuning within a smaller range (0.5 2 GHz/mA) can be achieved by modulating the driver current of the laser diode.

Most readily available DFB lasers are operating at one of the 15 wavelengths between 1310 and 1610 nm with 20 nm spacing defined by the International Telecommunications Union. It is possible to purchase them off-the-shelf for a few hundred euros housed in hermetically sealed butterfly package with an integrated thermoelectric cooler, thermistor, monitoring photodiode and a 30 dB optical isolator. The laser module we used in the setup is a 20 mW NEL NLK1556STB operating at a nominal wavelength of 1507.25 nm with a tuning range of ±4 nm and 2 MHz typical line width. It is housed in a 14-pin butterfly package, with a standard configuration of pins. The laser radiation is focused into a single-mode optical fiber ending with a FC/APC connector.

The high sensitivity of the emission frequency of the DFB laser to temperature or current changes calls for low-noise control electronics for applications that require high frequency stability.

We constructed the electronics self-containedly using only commercially available components and tools.

The current source, although conceptually simple, constitutes a tricky design problem. There is a number of practical requirements for a fiber optic current source and failure to consider them can cause laser and / or optical component destruction. Protection features must be included to prevent laser and optical component damage. The laser must be protected under all conditions, including supply ramp up and down and improper control input commands [20].

The current source that we constructed (Fig. 3) supplies up to 250 mA via Q1. This circuit requires both laser terminals to float. The amplifier controls laser current by maintaining the 1 shunt voltage at a potential dictated by the programming input. Local compensation at the amplifier stabilizes the loop and the 0.1 F capacitor filters input commands, ensuring the loop never slew limits. This precaution prevents overshoot due to programming input dynamics. The enable input turns off the current source by simultaneously grounding Q1's base and starving the amplifier's "+" input while biasing the "–" input high. This combination also ensures the amplifier smoothly ramps to the desired output current when enable switches low. Because the external circuitry operates from the

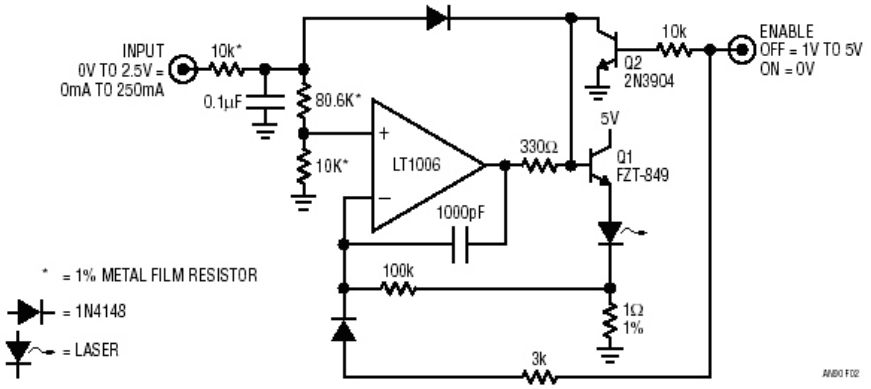

Fig. 3. The current source requires off-ground operation of laser terminals. Amplifier controls the current by comparing 1 shunt to input. Biasing enable, until supply is verified, prevents spurious outputs [20].

same 6V accumulator as the current source, the enable threshold is set at 1V. The 1V threshold ensures the enable input will dominate the current source output at low supply voltages during power turn on. This prevents spurious outputs due to unpredictable amplifier behavior below minimum supply voltage.

The laser module has an integrated thermoelectric cooler and a thermistor, thus it is sufficient for the temperature control of the laser chip to build a PID control unit in compliance with the electro-optical characteristics of the laser.

With our control electronics a long-term frequency stability of < 30 MHz was obtained without any additional locking scheme.

3. Results

3.1. Measurement of frequency stability

We measured the frequency stability of the setup by monitoring changes of the measured absorption at a set laser frequency.

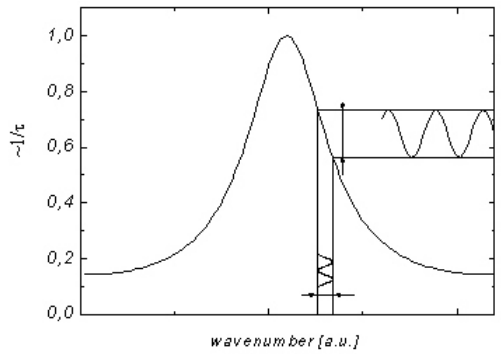

Fig. 4. The principle of measuring frequency stability by monitoring the changes of the measured absorption at a set laser frequency.

The laser was set to 6632.3 cm ^{1}. There are not any relevant atmospheric lines around this wavenumber: there should not be any changes in the measured exponential decay times caused be the fluctuation of the frequency of the laser.

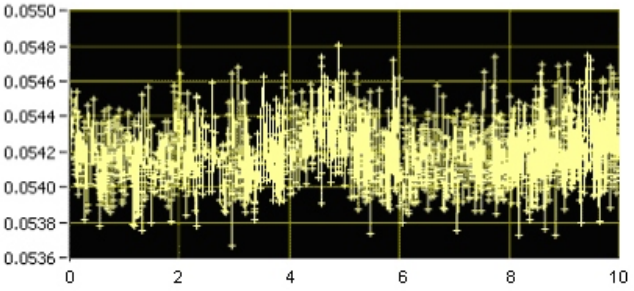

Fig. 5. 2500 measured values of 1/ ~ with the laser set to 6632.3 cm ^{1}.

2500 measured values of 1/ ~ (Fig. 5) show a noise level of 1.2 10 ^{3} s ^{1}. This corresponds to 4 10 ^{8} cm ^{1} change in absorption.

Without any other modifications the laser has been tuned to 6630.2 cm ^{1}, where the absorption line of water at 6630.0533 cm ^{1} is half height. At this point the fluctuation of the frequency of the laser should be reflected in fluctuations of the measured exponential decay times.

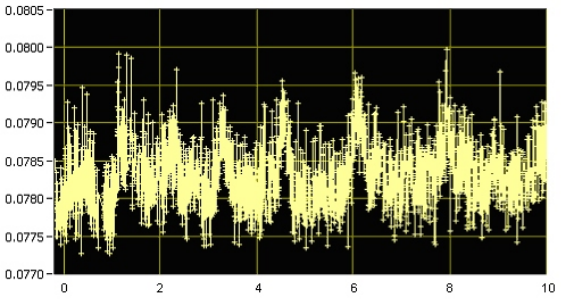

Fig. 6. 2500 measured values of 1/ ~ with the laser set to 6630.0533 cm ^{1}.

2500 measured values of 1/ ~ (Fig. 6) show a noise level 3 10 ^{3} s ^{1} which corresponds to 10 ^{7} cm ^{1} change in absorption.

The difference in the fluctuations of the measured absorption is 6 10 ^{8} cm ^{1}. From the slope of the absorption line at 6630.2 cm ^{1}, we calculated a corresponding fluctuation of 0.001 cm ^{1} (30 MHz) of the laser frequency.

3.2. The effect of mechanical vibrations

There is no patent experimental measure for controlling if the piezo expansion axis is in parallel with the optical axis of the cavity. If the piezo expansion axis is not aligned with the optical axis, it entails that with changing the laser wavelength, the position of the spot of the mirror, at which resonance occurs, also changes. As the coating of the mirrors is not perfectly uniform this systematically affects the cavity losses and introduces a systematical error into the measurements.

If there are mechanical vibrations introduced to the system, at a given laser wavelength resonance occurs with the same probability along the cavity modulation range and the spot of the mirror, at which resonance occurs, is also arbitrary. With subsequent averaging this noticeably lowers the noise level.

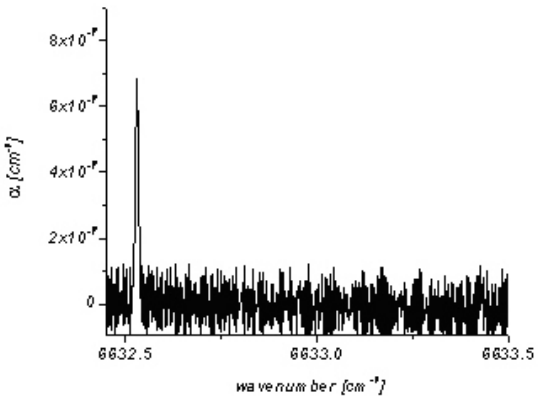

Fig. 7. Spectrum measured without mechanical vibrations.

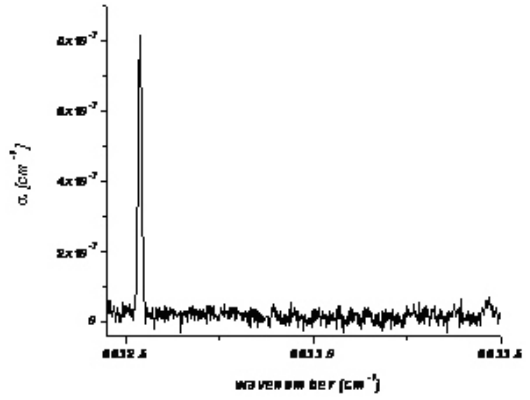

Fig. 8. Spectrum measured with mechanical vibrations induced by a hair blower fixed to the setup.

3.3. Atmospheric spectra

Atmospheric spectra from 6624 cm ^{1} to 6638 cm ^{1} were measured in flow regime 9.5 cm^3/min at 550 Pa pressure. We identified intensive water peaks at 6626.4772 cm ^{1}, 6627.7157 cm 1, 6628.909 cm ^{1}, 6630.053 cm ^{1}, 6634.5943 cm ^{1}. Less intensive peaks are also distinguishable up to 10 ^{8} cm ^{1}. The line profiles are given by Doppler broadening. The partial pressure of water was calculated to 5 Pa using line strengths from the HITRAN [21] database.

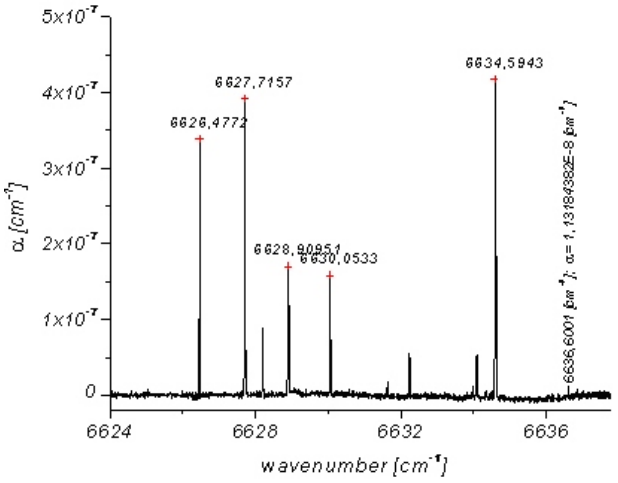

Fig. 9. Atmospheric spectra from 6624 cm ^{1} to 6638 cm ^{1}, measured in flow regime 9.5 cm^3/min at 550 Pa pressure.

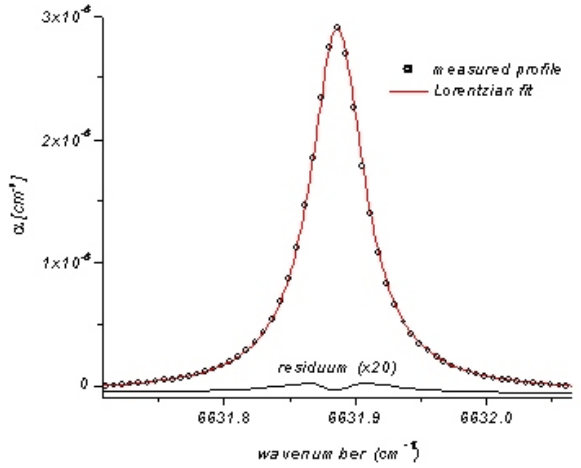

Fig. 10. Atmospheric absorption line of water at 6631.88 cm ^{1} fitted by Lorentz function, measured at atmospheric pressure.

The water peak in Fig. 8 was measured at atmospheric pressure and fitted by Lorentz function. The calculated partial pressure of water is 1671 Pa, which corresponds to 64 % relative humidity (at 21 C).

4. Discussion Upcoming Measurements Projects

In this paper we present sensitivity and variability of the CRDS system, which we have designed, built, and tested recently in our laboratory. The reason of its construction is to get sensitive detection system to detect small quantities of atoms, molecules, radicals, and ions. This technique can be used for solving mainly the following problems: Singlet oxygen study, study of radicals and radical chemistry (e.g. in microwave induced plasma).

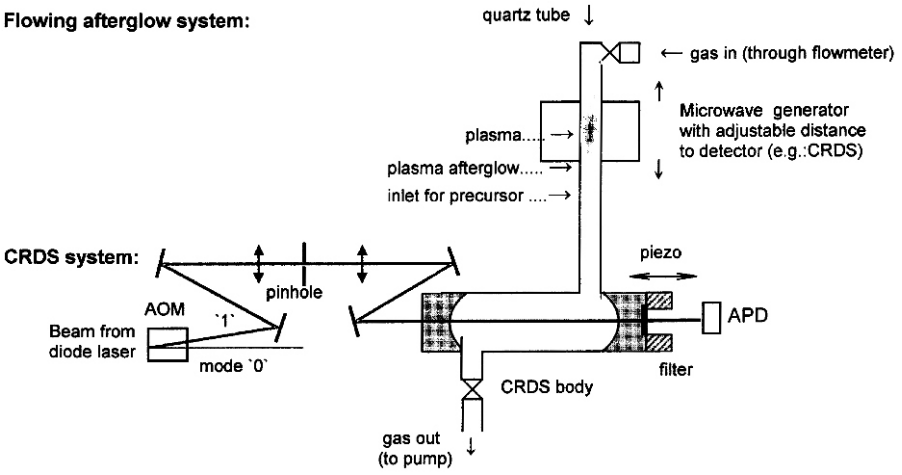

Fig. 11. Schematic view of the microwave flowing afterglow system with CRDS spectrometer.

In Fig. 11 we present our CRDS system for detecting species generated in microwave plasma (we chose a "clean" plasma source compared to e.g. DC discharge where electrodes are in a direct contact with the produced plasma and gas). In such an afterglow experimental apparatus excited radicals and transient molecules will be generated in the plasma afterglow and CRDS spectra will be analyzed. These experiments will help e.g. in the study of dynamics and kinetics of reactions in plasma between long living states of transient molecules and radicals to explain reaction steps in reactions that cannot be realized from ground states of radicals. It is assumed that they might be realized from the excited states but an experimental proof has not been given. Generation of excited state of radicals will be maintained in the afterglow region of the apparatus. The heart of the system consists of a quartz cavity placed through the cage of standard microwave oven (frequency 2.46 GHz, power 800 W) and connected perpendicularly to the CRDS body. Prior to making such a connection the part of microwave oven with maximal power must be chosen considering several segments of the oven by processing the map of the intensity profile of microwaves. We are designing and building a system, which will have the possi-

bility to generate plasma at different distances, since the microwave generator will be movable as pointed out in a schematic view (Fig. 11). Microwave generator can be modified so that there will be possibility to use it in both continual and pulsed regime.

Acknowledgements

We are indebted to Petr Hlavenka (Charles University) for his significant help with computer acquisition system. This research was sponsored by the Science and Technology Assistance Agency under the contract No. APVT-20-020204, by the Scientific Grant Agency of Slovak Republic VEGA 1/1016/04 and 1/2014/05. Flowing afterglow system is in a construction in the frame of VEGA 1/3043/06 project.

References

[1] W. Demtröder: Laser Spectroscopy, Springer-Verlag, Berlin (1998).
[2] A. O'Keefe, D. A. G. Deacon: Rev. Sci. Instrum. **59** (1988) 2544.
[3] R. D. Van Zee, J. T. Hodges, J. P. Looney: Appl. Opt. **38** (1999) 3951.
[4] T. G. Spence, C. C. Harb, B. A. Paldus, R. N. Zare, B. Willke, R. L. Byer: Rev. Sci. Instrum **71** (2000) 347.
[5] D. Romanini, A. A. Kachanov, N. Sadeghi, F. Stoeckel: Chem. Phys. Lett. **264** (1997) 316.
[6] R. Engeln, G. Von Helden, G. Berden, G. Meijer: Chem. Phys. Lett. **262** (1996) 105.
[7] P. Zalicki, R. N. Zare: J. Chem. Phys. **102** (1995) 2708.
[8] P. Macko, G. Bánó, P. Hlavenka, R. Plašil, V. Poterya, A. Pysanenko, O. Votava, R. Johnsen, J. Glosík: Int. J. Mass Spectr. **233** (2004) 299.
[9] P. Macko, G. Bano, P. Hlavenka, R. Plasil, V. Poterya, A. Pysanenko, K. Dryahina, O. Votava, J. Glosik: Acta Physica Slovaca **54** (2004) 263.
[10] A. Yalin: CRDS and applications to sputter measurements, CSU, May 6 2005.
[11] F. Grangeon, C. Monard, J. L. Dorier, A. A. Howling, C. Hollenstein, D. Romanini, N. Sadeghi: Plasma Sources Science & Technology 8, **3** (1999) 448.
[12] M. Murtz: Optics & Photonics News, publ. by Optical Society of America, January 2005, 30 35.
[13] D. Kleine, M. Murtz, J. Lauterbach, H. Dahnke, W. Urban, P. Hering, K. Kleinermanns: Israel Journal of Chemistry **41** (2001) 111.
[14] M. W. Todd, R. A. Provencal, T. G. Owano, B. A. Paldus, A. Kachanov, V. I. Vodopyanov, M. Hunter, S. Coy, J. I. Steinfeld, J. T. Arnold: Applied Physics B **75** (2002) 367.
[15] Sz. M. Tan, E. H. Wahl, A. Kachanov, B. Paldus: Photonics, October 2004.
[16] B. Fideric, R. A. Provencal, S. M. Tan, A. A. Kachanov, B. A. Paldus: Optics & Photonics News, publ. by Optical Society of America **7** (2003) 24.
[17] D. B. Atkinson: Analyst **128** (2003) 117.
[18] P. Hlavenka: Charles University in Prague, Faculty of Mathematics and Physics, Diploma Thesis: Study of Ion H^{3+} Recombination at Cryogen Conditions (in Czech) (2003).
[19] A. Deninger, T. Heine, F. Lison: TOPTICA Photonics AG, Spectroscopic Applications of Near-Infrared DFB Diode Lasers, Cleo Europe 2005, (2005).
[20] J. Williams: Linear Technology Corporation, Current Sources for Fiber Optic Lasers, A Compendium of Pleasant Current Events, Application Note 90, (2002).
[21] L. S. Rothman, A. Barbe, D. C. Benner, L. R. Brown, C. Camy-Peyret, M. R. Carleer, K. Chance, C. Clerbaux, V. Dana, V. M. Devi, A. Fayt, J.-M. Flaud, R. R. Gamache, A. Goldman, D. Jacquemart, K. W. Jucks, W. J. Lafferty, J.-Y. Mandin, S. T. Massie, V. Nemtchinov, D. A. Newnham, A. Perrin, C. P. Rinsland, J. Schroeder, K. M. Smith, M. A. H. Smith, K. Tang, R. A. Toth, J. Vander Auwera, P. Varanasi, K. Yoshino: The HITRAN Molecular Spectroscopic Database: Journal of Quantitative Spectroscopy & Radiative Transfer **82** (2003) 5 44.